

<b>Project acronym:</b>	<b>GeoHex</b>		
<b>Project title:</b>	Advanced material for cost-efficient and enhanced heat exchange performance for geothermal application		
<b>Activity:</b>	LC-CS3-RES-1-2019-2020 Developing the next generation of renewable energy technologies		
<b>Call:</b>	H2020-LC-CS3-2019-RES-TwoStages		
<b>Funding Scheme:</b>	RIA	<b>Grant Agreement No:</b>	851917
<b>WP1</b>	Requirement analysis and project mapping		

### D1.4 Ideal Condensing surface for water and ORC fluid

<b>Due date:</b>	29/02/2020	
<b>Actual Submission Date:</b>	28/02/2020	
<b>Lead Beneficiary:</b>	TWI	
<b>Main authors/contributors:</b>	Imran Bhamji, Alan Taylor	
<b>Dissemination Level<sup>1</sup>:</b>	PU	
<b>Nature:</b>	Others	
<b>Status of this version:</b>		<b>Draft under Development</b>
		<b>For Review by Coordinator</b>
	X	<b>Submitted</b>
<b>Version:</b>	V1	
<b>Abstract</b>	This deliverable reports on the Ideal Condensing surface for water and ORC Fluid	

### REVISION HISTORY

Version	Date	Main Authors/Contributors	Description of changes



This project has received funding from the European Union's Horizon 2020 Research and Innovation programme under grant agreement No. 851917

<sup>1</sup> Dissemination level security:

**PU** – Public (e.g. on website, for publication etc.) / **PP** – Restricted to other programme participants (incl. Commission services) /

**RE** – Restricted to a group specified by the consortium (incl. Commission services) / **CO** – confidential, only for members of the consortium (incl. Commission services)

*This project has received funding from the European Union's Horizon 2020 program Grant Agreement No 851917. This publication reflects the views only of the author(s), and the Commission cannot be held responsible for any use which may be made of the information contained therein.*

**Copyright © 2019-2022, GeoHex Consortium**

This document and its contents remain the property of the beneficiaries of the GeoHex Consortium and may not be distributed or reproduced without the express written approval of the Geo-Drill Coordinator, TWI Ltd. ([www.twi-global.com](http://www.twi-global.com))

*THIS DOCUMENT IS PROVIDED BY THE COPYRIGHT HOLDERS AND CONTRIBUTORS "AS IS" AND ANY EXPRESS OR IMPLIED WARRANTIES, INCLUDING, BUT NOT LIMITED TO, THE IMPLIED WARRANTIES OF MERCHANTABILITY AND FITNESS FOR A PARTICULAR PURPOSE ARE DISCLAIMED. IN NO EVENT SHALL THE COPYRIGHT OWNER OR CONTRIBUTORS BE LIABLE FOR ANY DIRECT, INDIRECT, INCIDENTAL, SPECIAL, EXEMPLARY, OR CONSEQUENTIAL DAMAGES (INCLUDING, BUT NOT LIMITED TO, PROCUREMENT OF SUBSTITUTE GOODS OR SERVICES; LOSS OF USE, DATA, OR PROFITS; OR BUSINESS INTERRUPTION) HOWEVER CAUSED AND ON ANY THEORY OF LIABILITY, WHETHER IN CONTRACT, STRICT LIABILITY, OR TORT (INCLUDING NEGLIGENCE OR OTHERWISE) ARISING IN ANY WAY OUT OF THE USE OF THIS DOCUMENT, EVEN IF ADVISED OF THE POSSIBILITY OF SUCH DAMAGE*

## CONTENTS

1	EXECUTIVE SUMMARY .....	4
2	OBJECTIVES MET .....	4
3	SEARCH METHODOLOGIES .....	4
4	INTRODUCTION .....	6
4.1	OVERVIEW .....	6
4.2	DROPWISE VS FILMWISE CONDENSATION .....	6
5	SURFACE ENERGY AND WETTING BEHAVIOUR .....	7
5.1	SURFACE ENERGY.....	7
5.2	TOPOGRAPHIC CONSIDERATIONS.....	11
5.3	CONTACT ANGLE HYSTERESIS.....	13
5.4	SUMMARY .....	16
6	SELECTION OF RELEVANT PARAMETERS AND CORRELATIONS FOR DWC OPTIMISATION .....	16
7	SCIENTIFIC LITERATURE ON SUPERHYDROPHOBIC COATINGS .....	18
7.1	OVERVIEW .....	18
7.2	ROUGHNESS GENERATION: TOP-DOWN/BOTTOM UP APPROACHES .....	18
7.3	STEEL SUBSTRATES.....	19
7.4	COPPER SUBSTRATES.....	21
7.5	ALUMINIUM SUBSTRATES.....	21
8	ENHANCEMENT METHODS SPECIFIC TO GEOHEX.....	22
8.1	SUPERHYDROPHOBIC AND SUPEROLEOPHOBIC SURFACES WITH CUO NANOSTRUCTURES .....	22
8.2	SUPERHYDROPHOBIC AND SUPEROLEOPHOBIC SURFACES WITH TiO <sub>2</sub> /ZNO NANOPARTICLES FOR CONDENSATION.....	22
8.3	FUNCTIONAL HIERARCHICAL MESH-COVERED SURFACES .....	22
8.4	ROBUST HYDROPHOBIC/OLEOPHOBIC AMORPHOUS METAL COATINGS .....	24
9	SUMMARY .....	25
10	REFERENCES.....	26

## **1 EXECUTIVE SUMMARY**

The GeoHex project aims to develop advanced materials to allow for the cost efficient improvement in heat exchanger performance for geothermal energy sources. The overarching need is to facilitate growth in the adoption of geothermal energy to allow the EU to achieve its decarbonisation objectives and climate change mitigation targets.

The basis of the GeoHex concept is the development of new materials that lead to reduced scaling and corrosion while also improving heat transfer properties. It is anticipated that the development of such materials will lead to smaller, more efficient and lower cost systems.

A central tenet of the research strategy of the GeoHex project is that heat transfer performance of dropwise condensation is several times higher than conventional film wise condensation. Nucleate boiling provides similar benefits when compared with film boiling. This literature review will be informative for WP3, which will focus on the development of materials for organic Rankine cycle (ORC) and steam condensers that promote droplet formation as opposed to film forming of ORC working fluids such as hydrocarbons, fluorocarbon refrigerants and, of course, water.

This report is a review of the underpinning science behind the wetting of solid surfaces by liquids and approaches to the generation of the non-wetting behaviour that leads to droplet rather than film formation. The intertwined factors of interfacial chemistry and surface topography will be examined together with a short review of the current state-of-the-art with particular reference to ultralow surface tension liquids such as 1,1,1,2-tetrafluoroethane (also known as R134a), which has been identified as a candidate refrigerant in the GeoHex project.

## **2 OBJECTIVES MET**

- Characterise ideal condensing surface for low surface tension fluid and steam.

## **3 SEARCH METHODOLOGIES**

Literature searches were performed using Scopus; a list of the search terms is included in Table 1. Some broad searches gave rise to more papers than could be reasonably reviewed, so narrower search terms were used. This may have led to some papers of relevance not being reviewed in this report.

Table 1 List of search terms

Index	Search String	Hits
1	TITLE-ABS-KEY ( condensation AND (coating* OR surfac* ) )	33176
2	TITLE-ABS-KEY ( condensation AND ( coating* OR surfac* ) AND ( "drop wise condensation" OR "dropwise condensation" OR dwc OR ( drop W/3 condensation ) ) )	980
3	TITLE-ABS-KEY ( ( "drop wise condensation" OR "dropwise condensation" OR dwc ) AND condensation AND ( coating* OR surfac* ) AND ( "contact angle" ) AND ( "chemical vap* deposition" OR cvd OR "chemical vap* deposition" OR cu ) )	16
4	TITLE-ABS-KEY ( ( "drop wise condensation" OR "dropwise condensation" OR dwc ) AND condensation AND ( coating* OR surfac* ) AND ( "contact angle" ) AND ( nanoporous OR "nano porous" ) )	2
5	TITLE-ABS-KEY ( ( "drop wise condensation" OR "dropwise condensation" OR dwc ) AND condensation AND ( coating* OR surfac* ) AND ( "contact angle" ) AND ( ( zinc W/3 ox* ) OR zno ) )	1
6	TITLE-ABS-KEY ( ( "drop wise condensation" OR "dropwise condensation" OR dwc ) AND condensation AND ( coating* OR surfac* ) AND ( "contact angle" ) AND ( carbon W/3 nano* OR carbonnano* ) )	4
7	TITLE-ABS-KEY ( ( "drop wise condensation" OR "dropwise condensation" OR dwc ) AND condensation AND ( coating* OR surfac* ) AND ( "contact angle" ) AND ( ( iron W/3 ox* ) OR feo OR fe2o3 OR fe3o4 ) )	0
8	TITLE-ABS-KEY ( ( "drop wise condensation" OR "dropwise condensation" OR dwc ) AND condensation AND ( coating* OR surfac* ) AND ( "contact angle" ) AND ( ( copper W/3 ox* ) OR cuo OR cu2o OR cu2o3 ) )	13
9	TITLE-ABS-KEY ( ( "drop wise condensation" OR "dropwise condensation" OR dwc ) AND condensation AND ( coating* OR surfac* ) AND ( "contact angle" ) AND ( ( titanium W/3 ox* ) OR tio OR tio2 OR ti2o3 ) )	1
10	TITLE-ABS-KEY ( ( "drop wise condensation" OR "dropwise condensation" OR dwc ) AND condensation AND ( coating* OR surfac* ) AND ( "contact angle" ) AND ( amorphous OR ( metallic W/3 glass ) ) )	1
11	TITLE-ABS-KEY ( condensation AND ( coating* OR surfac* ) AND ( "drop wise condensation" OR "dropwise condensation" OR dwc OR ( drop W/3 condensation ) ) AND ( amorphous OR ( metallic W/3 glass ) ) )	6

## 4 INTRODUCTION

### 4.1 Overview

The wetting of solids by liquids is, of course, of significant importance in both the natural and industrial worlds. Excellent wetting is a pre-requisite for processes such as bonding and coating, while non-wetting is essential to maintain a pristine surface or to promote droplets rather than film-formation. This is especially relevant to condensation heat transfer. Phase change leads to a large heat transfer due to a change in the latent heat, which can lead to high levels of heat transfer through condensation (Miljickovic and Wang, 2017). The amount of wetting is a key parameter in the efficiency of condensation heat transfer.

The wettability of surfaces is governed both by chemical and structural considerations and there are many excellent review articles on the chemistry and physics of wetting and particularly non-wetting (Shirtcliffe et al, 2004; Quéré and Reyssat, 2008; Ma and Hill, 2006).

### 4.2 Dropwise vs filmwise condensation

The efficiency of condensation phase change heat transfer is greatly enhanced by dropwise condensation (DWC), as was first theorised by Schmidt et al. (1930), compared to filmwise condensation (FWC). It is therefore desirable to promote DWC on surfaces where condensation heat transfer is required to be maximised, for example, in heat exchanger systems. In DWC, liquid drops form at a surface that is cool with respect to the surrounding environment. Over time, more and more droplets form, with a tendency to coalesce to form larger droplets. If the droplets are able to leave the surface reasonably rapidly, this will allow DWC to continue in a stable manner; the surface area freed by droplet departure can nucleate new droplets (Bisetto et al, 2014). However, if the droplets remain on the surface until they reach the condensate capillary length, they will tend to flow together to form a film, leading to FWC. This significantly increases the thermal resistance at the interface, reducing the heat transfer properties. Therefore, stable DWC is dependent on a surface which allows the formation and rapid removal of droplets.

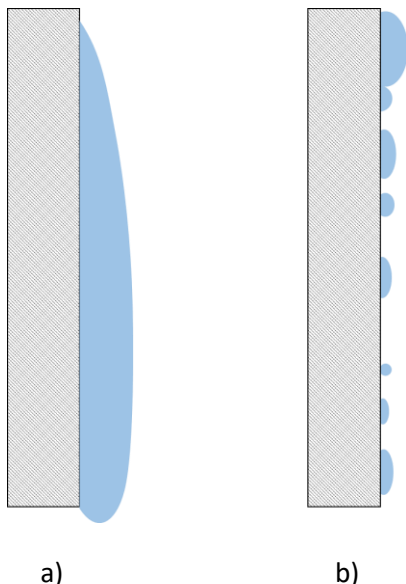


**Figure 1** Schematic illustrating filmwise (a) vs dropwise (b) condensation

Promotion of DWC is dependent on a number of factors. Minimising the surface energy will tend to increase the contact angle of droplets on the surface, giving rise to a hydrophobic surface which stabilises DWC (Ranieri et al, 2009; Bisetto et al, 2014). Similarly, a higher liquid surface tension achieves a similar effect. A greater

difference in temperature between the vapour and wall temperature will increase the density of nucleation sites; but droplets will tend to coalesce and act to promote FWC (Khan et al, 2019). DWC is therefore harder to sustain on a surface with a greater degree of supercooling. The roughness of the condensation surface is also a key factor. The durability of coatings and surfaces should also be considered, as many coatings, which give rise to DWC, breakdown over time or are easily damaged.

Therefore, this review will report on techniques used to promote DWC. Maximising the hydrophobicity of a surface is a key factor, which will be discussed in depth, alongside using micro or nano-structuring to produce super hydrophobic surfaces. Specific examples relevant to GeoHex will also be considered, in relation to reported effects on the resultant condensation and heat transfer behaviour. Correlations for different parameters of droplet dynamics will also be selected which will be used to validate the simulation tools and image processing algorithm (WP6) related to droplet dynamics.

## 5 SURFACE ENERGY AND WETTING BEHAVIOUR

### 5.1 Surface energy

The molecular arrangement of a solid, liquid or gas has a number of implications and particularly thermodynamic considerations. For solids and liquids the surface represents a higher energy state, in comparison with the bulk, since the molecular arrangement is disrupted and therefore bonds are strained. Liquids have the opportunity to reduce their surface energy by reducing their surface area by forming spheres; solids do not have this capability. The interface between a liquid and a solid is dependent on a range of factors; assuming no chemical reactivity the dominant factor is the relative energies of the surface of the liquid and solid with due consideration to the vapour phase.

In the nineteenth century the wetting behaviour of solids by liquids (mainly water) was studied in some detail (Young, 1805) and the foundations for surface energy measurement and determination were established.

The interaction between the liquid and the solid surface in terms of the ability of the liquid to wet is described by the Young equation:

$$\gamma_S = \gamma_L \cdot \cos\theta + \gamma_{SL} \quad [1]$$

Where  $\gamma_S$  is the surface energy of the solid,  $\gamma_L$  is the surface energy of the liquid and  $\gamma_{SL}$  is the surface energy at the interface between the solid and liquid, this assumes the vapour phase is always air. The angle,  $\theta$ , is the contact angle between the liquid droplet and the solid as shown in Figure 2.

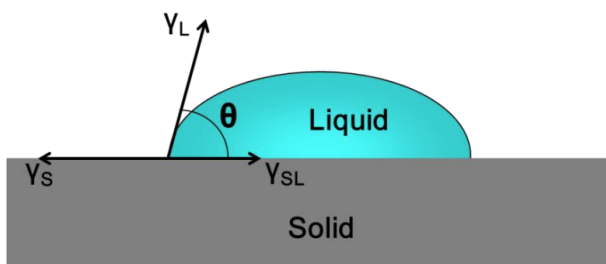
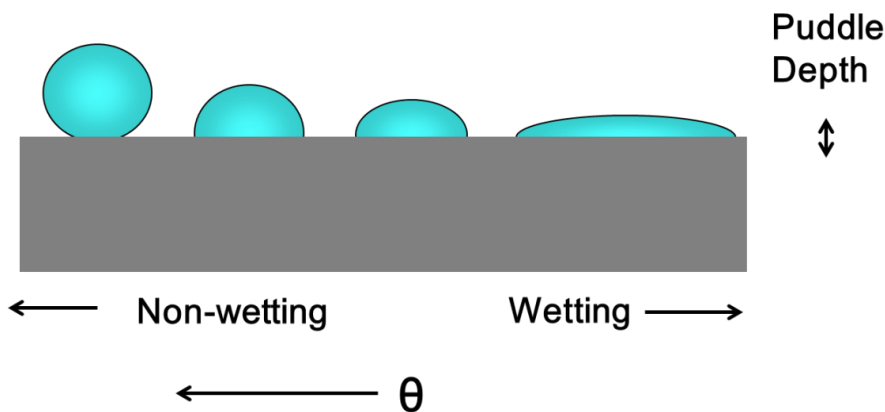


Figure 2 Contact angle and wettability.

For a given liquid, as the surface energy of the solid reduces the contact angle increases. This is shown in Figure 3, for droplets of similar volume.



**Figure 3** Schematic relationship between wettability and contact angle.

The nomenclature for describing wetting behaviour has yet to be standardised, but some descriptions and definitions are widely accepted (Marmur, 2012) and are based on contact angle ( $\theta$ ) measurements. The below are specifically for the condition when the liquid is water, but related terms for oils and fats or even just for liquids, in general, exist.

- Hydrophilic when  $0^\circ \leq \theta < 90^\circ$ .
- Hydrophobic when  $90^\circ \leq \theta < 150^\circ$ .
- Superhydrophobic when  $\theta \geq 150^\circ$ .

The underpinning theoretical framework behind the concept of solids having a surface energy is a matter of considerable debate (Makkonen, 2016) in the scientific literature. However, in practice it is useful to have a value that allows comparison; it is also common practice to use static contact angles to illustrate the wetting of surfaces by liquids. The most commonly reported contact angle is that with water; this is frequently abbreviated to WCA (water contact angle). Table 2 gives the WCA values of a number of surfaces (Arkles B., 2006). The ability of a surface to shed liquids is dependent on the surface energy (ElSherbini and Jacobi, 2006; Extrand and Gent, 1990; Extrand and Kumagai, 1995), but also how this property is constructed.

**Table 2** WCA values for various surfaces

Surface/surface treatment	Water contact angle
Poly(tetrafluoroethylene)	108-112°
Poly(propylene)	108°
Octadecyldimethylchlorosilane	110°
Trimethylchlorosilane	90-100°
Poly(ethylene)	88-103°
Poly(styrene)	94°
Human skin	75-90°
Diamond	87°
Silicon (etched)	86-88°
Talc	50-55°
Steel	70-75°
Gold, typical	66°
Platinum	40°
Silicon nitride	28-30°
Silver iodide	17°
Soda-lime glass	<15°

This table is interesting from two perspectives. The first is that fluorinated surfaces or fully reacted hydrocarbons give the highest water contact angles. The second is that these values relate to smooth surfaces. Therefore, from a chemical perspective the highest WCA that can be achieved is approximately 112°. This is at slight variance with more detailed studies (Lee et al, 2008) but there appears to be an upper limit for the WCA of ~120° for planar surfaces.

The contact angle,  $\theta$ , and the surface energy of the liquid  $\gamma_L$ , can be readily measured, but the surface energy of the solid,  $\gamma_S$  and interfacial energy between solid and liquid cannot. However, a theoretical framework has been developed that allows the estimation of these factors.

The work required to separate two phases as a function of the surface energies of each phase and defined the following relationship:

$$W_{SL} = \gamma_S + \gamma_L - \gamma_{SL} \tag{2}$$

Where  $W_{SL}$  is often referred to as the work of adhesion. Combining Equations [1] and [2] yields the Young-Dupr e relationship:

$$W_{SL} = \gamma_L(1 + \cos\theta) \tag{3}$$

The work of cohesion is defined as when  $\gamma_{sl} = 0$ , that is when the work necessary to separate the two phases is only dependent on their relative surface energies such as when the two phases are identical.

$$W_C = \gamma_S + \gamma_S - 0 = 2\gamma_S \quad [4]$$

Berthelot introduced the idea that the work of adhesion was equal to the geometric mean of the cohesion work of the solid and the liquid. That is:

$$W_{SL} = \sqrt{W_S W_L} \quad [5]$$

Which can be rewritten as:

$$W_{SL} = 2\sqrt{\gamma_S \gamma_L} \quad [6]$$

Combining Equations [3] and [6] yields the relationship:

$$\gamma_L(1 + \cos\theta) = 2\sqrt{\gamma_S \gamma_L} \quad [7]$$

This suggests that the surface energy of a solid can be determined from the measurement of the contact angle of a single liquid, as long the surface energy of the liquid is known.

Further work, initially by Fowkes (1964) and then by others expanded on these ideas by introducing considerations of dispersive, polar, hydrogen, induction and acid-base bonding.

These terms are assumed to sum together to provide the cumulative term for the surface energy of the solid (or liquid):

$$\gamma_S = \gamma_S^d + \gamma_S^p + \gamma_S^h + \gamma_S^i + \gamma_S^{ab} \quad [8]$$

A primary contribution (Owens and Wendt, 1969) was to determine that all the forces with the exception of the dispersive forces (which arise from electron dipole fluctuations) can be considered to be polar. This therefore leads to equation 9:

$$\gamma_{sl} = \gamma_S + \gamma_L - 2\sqrt{\gamma_S^d \gamma_L^d} - 2\sqrt{\gamma_S^p \gamma_L^p} \quad [9]$$

Combining Equation [9] with Equation [1] yields the OWRK (Owens, Wendt, Rabel and Kaelble) equation, also called the extended Fowkes equation, which is the basis for most surface energy measurements.

$$2\sqrt{\gamma_S^d \gamma_L^d} - 2\sqrt{\gamma_S^p \gamma_L^p} = 0.5\gamma_L(1 + \cos\theta) \quad [10]$$

There are two unknown terms in this equation  $\gamma_S^d$  and  $\gamma_S^p$ , the disperse and polar terms respectively of the surface energy of the solid. To determine the value of these two terms two liquids with known polar and dispersive values are used. The liquids are selected to ensure that one is dominant from a polar perspective and the other from a dispersive. Typically, diiodomethane is used as one of the liquids as this has no polar component and so it is assumed dispersive forces dominate its surface characteristics. The second liquid (often water) is highly polar. This approach allows Equation [10] to be solved algebraically, since the polar and disperse values of these liquids are well known and can be readily calibrated. The most common methods employed to determine the surface energy of solids are summarised in Table 3.

**Table 3** Common methods for determining the surface energy of a solid.

Method	Characteristics	Comments
Zisman: Critical surface energy	Maximum surface tension a liquid may have to ensure complete wetting	Used as a wettability benchmark; solids possessing a high critical surface energy are readily wetted by most liquids
Fowkes or OWRK method	Total surface energy and its components derived using the geometric mean.	Suitable for characterisation of non-polar and moderately polar substrates such as plastics, rubber, polymer films, paper, etc.
van Oss-Good: the acid-base method	Total surface energy; dispersive, polar, acid and base parameters.	A modification of the OWRK method better suited for the characterisation of polar substrates, e.g. polyacrylamides, proteins, mineral surfaces, which are likely to be engaged in acid-base interactions with highly polar test liquids.
Harmonic mean (aka the Wu method)	Total surface energy and its components derived using the harmonic mean	Similar to OWRK method.
Li-Neumann: the equation of state method	Total surface energy derived using the equation of state	Suitable for characterisation of non-polar and moderately polar substrates such as plastics, rubber, polymer films, paper, etc. The preferred method if the polarities of the substrate and of the test liquids differ significantly.

## 5.2 Topographic considerations

Surface energy calculations that ultimately derive from Young’s equation (Equation [1]) are fundamentally built on the assumption that the surface is planar and therefore there is no impact from surface texture on the measured contact angle.

However, most solids have some texture and so a modification of Young’s equation was developed to account for surface roughness, Equation [11] (Wenzel, 1936). This model describes a homogeneous wetting regime. The wetting model assumes that the liquid is in complete contact with the solid and it makes it harder for the drop to roll off due to the larger contact area. (Li et al, 2016). The Wenzel wetting is described by Equation [11] below:

$$\cos(\theta_w) = r \cos \theta_Y \tag{11}$$

Where,  $\theta_w$  is the apparent contact angle, and  $\theta_Y$  is the intrinsic (Young) contact angle. The value  $r$  is the roughness ratio and is defined below

$$r = \text{roughness factor} = \frac{\text{actual surface area}}{\text{planar surface area}} \quad [12]$$

The relationship suggested by Wenzel predicts that roughness enhances the wetting behaviour of a solid since it makes a hydrophilic surface even more hydrophilic and a hydrophobic surface even more hydrophobic. This is shown graphically in Figure 4.

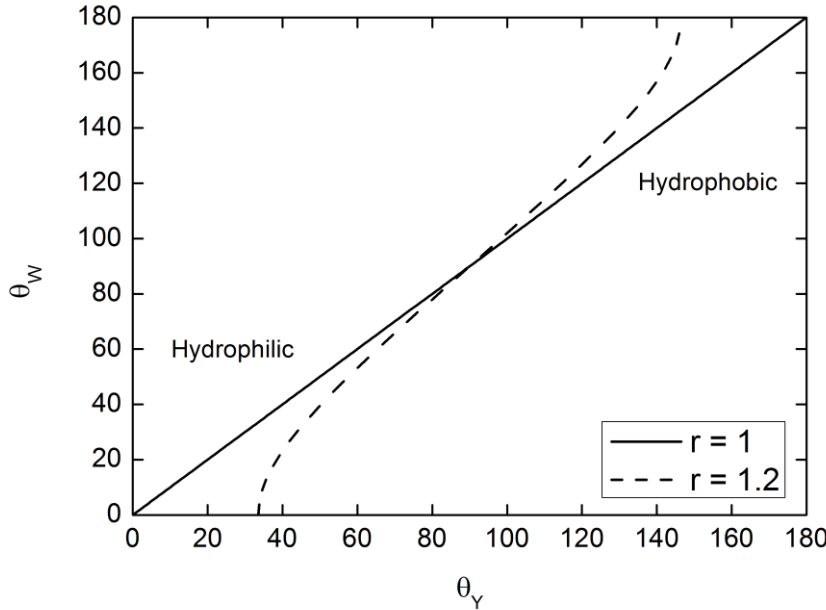


**Figure 4** Impact of roughness factor on the apparent contact angle.

The Wenzel model assumes chemical homogeneity and that the liquid penetrates all the roughness grooves on the solid surface. An alternative model was developed to account for chemical inhomogeneity (Cassie and Baxter, 1944). This model considers the area occupied by multiple ( $n$ ) chemically distinct regions as a function of the total area and the intrinsic characteristics of each. In this scenario, if we consider the fraction associated to each material and we introduced it in Young's equation where  $\gamma_S \rightarrow \sum_i^n f_i \cdot \gamma_{iS}$  and  $\gamma_{SL} \rightarrow \sum_i^n f_i \cdot \gamma_{iSL}$ , this leads to the Cassie-Baxter equation;

$$\cos \theta_{CB} = \sum_i^n f_i \cdot \cos \theta_{iY} \quad [13]$$

This equation therefore relates the measured (apparent) contact angle to the intrinsic contact angles and takes into account the fraction ( $f_i$ ) of each material that composes the surface of the solid and is in contact with the liquid. The equation can therefore be simplified to the following if the surface is assumed to consist of two distinct chemical regions (which may be randomly dispersed).

$$\cos \theta_{CB} = f_1 \cos \theta_{1Y} + f_2 \cos \theta_{2Y} \quad [14]$$

The Wenzel and Cassie-Baxter state can transition into each other under some conditions. This approach has been widely adopted to explain very high levels of measured contact angle that can occur with highly structured surfaces. The surface can be considered as a composite of the solid material and entrapped air between the peaks of the solid, Figure 5.

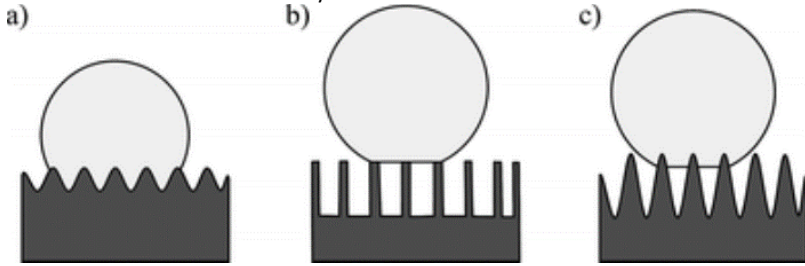


Figure 5 Wetting states: Young's, Wenzel and Cassie-Baxter.

Distinguishing between Wenzel and Cassie-Baxter wetting is typically done empirically. If a drop of liquid is placed on a solid surface and it easily slides, the Cassie Baxter regime applies. However, if the droplet sticks to the surface even though it is nominally hydrophobic the Wenzel regime applies.

### 5.3 Contact angle hysteresis

Whether a droplet adheres or readily moves is probably the single most important factor in determining the functional properties of a surface. Unless the surface is perfectly flat and horizontal, the droplet will exhibit a range of contact angles around the mean value  $\theta_Y$ . When viewed in profile, the two extremes are conventionally referred to as the advancing and receding contact angles, Figure 6.

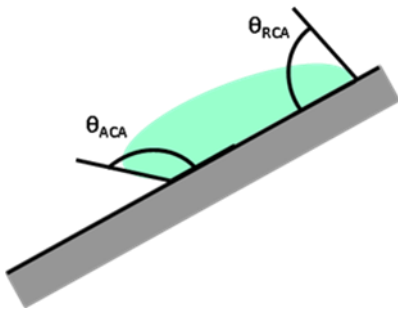


Figure 6 Advancing (ACA) and receding (RCA) contact angles for a liquid drop on a tilted substrate.

Contact angle hysteresis and the tilting angle ( $\alpha$ ) when the droplet rolls off (widely known as the roll-off angle) are often used as measures of how repellent a surface is to liquids. When droplets move more readily this correlates with lower values for the hysteresis and roll-off angle. In this circumstance, it is easier for the droplet to move rather than to deform and form a film with a greater interfacial contact area.

Numerous studies have been undertaken to understand the origins of contact angle hysteresis, however, no general agreement on the mechanics that underpin these behaviours has yet been reached (Makkonen, 2017).

As a droplet moves, for example under the force of gravity, it deforms, bulging at the advancing front edge and trailing at the receding line. This state gives us a maximum value for the sticking force (Krasovitski and Marmur, 2005). The force per unit of length acting on the receding angle of the drop is:

$$F_r = \gamma_{SV} - \gamma_{SL} - \gamma_{LV} \cos \theta_r \quad [15]$$

The force acting on the advancing part is:

$$F_a = \gamma_{SV} + \gamma_{LV} \cos \theta_a - \gamma_{SL} \quad [16]$$

Thus, the maximum adhesive force can be derived as:

$$F = \gamma_{Lv}(\cos \theta_r - \cos \theta_a) \quad [17]$$

If this force is integrated along the contact line the following equation will be derived for the sticking force:

$$F = \pi\gamma_{Lv}R \sin \theta (\cos \theta_r - \cos \theta_a) \quad [18]$$

Where, R is the radius of curvature of the droplet. Droplets move more easily along the surface of the solid when the contact angle hysteresis is minimised and therefore the average contact angle between the solid and the liquid is at a maximum (Quéré and Reyssat, 2008). If it is energetically favourable for the droplet to spread on the solid surface, increasing the interfacial area rather than to maintain its shape, the droplet will deform and the contact angle hysteresis will increase. As more energy is applied to the droplet (as the tilting angle of the solid increases and the applied gravitational force increases for example) the contact area increases until it becomes energetically favourable for the droplet to move rather than to continue to spread. The energetic argument from the perspective of spreading is widely accepted but is still the subject of some debate; an alternate view is that the receding edge of the droplet is pinned by very local factors. In this model the droplet will continue to deform until the force acting on the droplet is greater than the pinning force.

Johnson and Dettre (1964) reported the changes in contact angle and contact angle hysteresis as a function of surface roughness. As surface roughness increased so did the observed contact angles and the hysteresis decreased until it was practically negligible.

The most widely recognised example of superhydrophobicity is the lotus leaf. The underpinning morphology behind this behaviour is dual scale roughness (Koch and Bartholt, 2009), with a hydrocarbon surface chemistry that is hydrophobic. Quéré and Reyssat (2002) examined repellent rough surfaces and concluded that dual scale roughness (Figure 7) enhances the repellence and this can be understood by the fact that while Van der Waals forces reinforce the Wenzel wetting, the Cassie-Baxter state will be achieved if there is an air-liquid interface preventing such interactions.

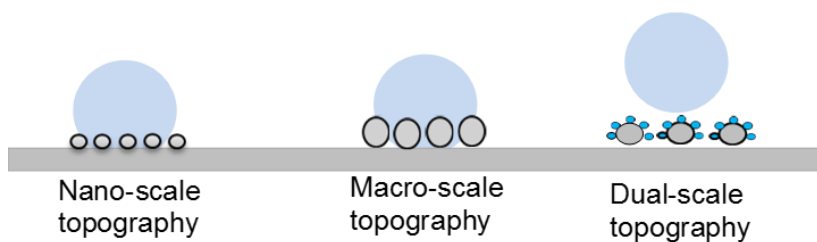


**Figure 7** Schematic of different types of roughness

The role of nanoscale roughness is therefore to introduce a capillary pressure which resists filling and so stabilises the air-liquid interface. Quéré and Reyssat (2002) derived the relationship between the contact angle hysteresis sticking force (Equation [18]) and the capillary force. The capillary force can be calculated by the following equation:

$$F_k = \pi b \gamma_{LV}(\cos \theta_r - \cos \theta_a) \quad [19]$$

Where,  $b$  is the radius of the liquid contact with the solid surface and this is related to the capillary length,  $k$  by the following relationship:

$$b \sim R^2 k \tag{20}$$

Where  $k$  is:

$$\frac{1}{k} = \left( \frac{\gamma_{LV}}{\rho g} \right)^{0.5} \tag{21}$$

Considering this in more detail, the capillary rise of a liquid in the tube, the height ( $h$ ) gained by the liquid can be determined by the equilibrium contact angle. If the liquid wets the solid (the surface energy of the solid is greater than the surface tension of the liquid), the liquid rises up to the height at which the interfacial surface tension balances the weight of the raised liquid in the capillary. The height of the raised liquid can be calculated using Jurin's height equation (Lautrup, 2010):

$$h = 2 \frac{k}{a} \cos \theta \tag{22}$$

Where  $k$  is capillary length and  $a$  is radius of the tube.

According to Quéré and Reyssat (2002), the contact of the liquid with the solid is dependent on the size of the droplet. If the gravitation force applied by the droplet overcomes the pressure of the capillary to resist filling, the droplet will adhere to the surface. If however, the capillary pressure to resist filling is greater than the applied force on the droplet to fill the capillary the air will remain in the capillary. In this case, the air-liquid interface prevents van der Waals interactions and the adhesion force between the droplet and the surface is minimised so the droplet can readily move.

Capillary forces can make it difficult for the liquid to penetrate into the roughness of the coating or the surface. In this case, energetically it is favourable for a liquid to adopt the Cassie-Baxter state rather than to be conformal as described by Wenzel.

Returning to Equation [3], allows the work of adhesion as a function of contact angle to be drawn, Figure 8.

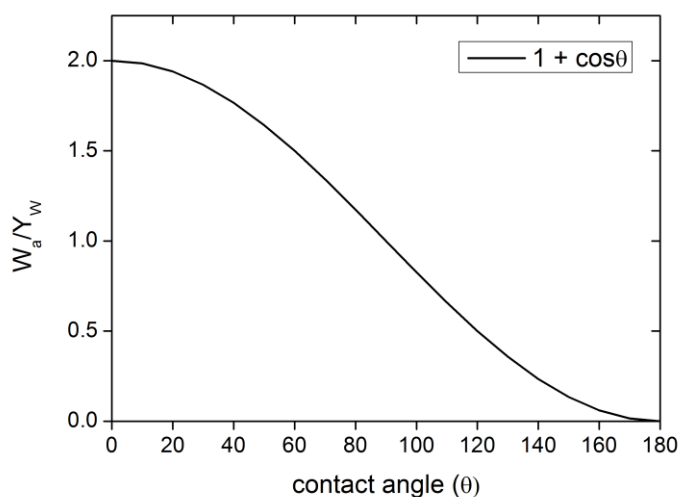


Figure 8 Work of adhesion to remove a liquid droplet from a solid surface as a function of the contact angle,  $\theta$ .

## 5.4 Summary

The Young equation is the starting point for most descriptions of wetting/non-wetting behaviour. Explicit within this approach is the assumption that if a liquid has a lower surface energy than the solid it will wet the surface. Conversely, if the solid has a lower surface energy than the surface tension of the liquid, the liquid will tend towards beading rather than forming a film. The larger the difference in the surface energy values of the liquid and solid the more pronounced these effects. Modification of the chemistry of surfaces can reduce their surface energy. This is most typically done by the use of ligands with low potential for reaction and low capability for hydrogen bonding. Examples include olefin polymers, silicones and fluorocarbons. However, as discussed earlier, minimising the surface energy via solely chemical methods is limited in how much increase in contact angle can be achieved, and therefore how much the work of adhesion between the liquid and the surface can be reduced. Further reduction in the adhesion between the solid and liquid therefore can only be accomplished via the introduction of topographic features. The description that is often used to help convey the desired functionality is the lotus effect, so many approaches to generate roughness are discussed as being bio-mimetic. The high surface tension value of water means the conditions for superhydrophobic behaviour are met by many combinations of surface roughness and chemistry. However, it is still far from clear which specific topographic features are required to achieve high levels of repellence of liquids with much lower surface tension values. All of these factors are highly significant to promote dropwise condensation to enhance condensation heat transfer.

## 6 SELECTION OF RELEVANT PARAMETERS AND CORRELATIONS FOR DWC OPTIMISATION

A number of parameters are key to assess and model DWC behaviour, as expressed in literature (Abu-Orabi, 1998; Sikarwar et al, 2013). These include the following:

- $r_f$ : Degree of roughness (subscript f to distinguish from droplet radius, r)
- r: Droplet radius
- $\Theta$ : Droplet contact angle

Other key constants or variable include:

- $q_d$ : Heat transfer
- k: Thermal conductivity of material
- $T_{sat}$ : Vapour saturation temperature
- $T_w$ : Wall temperature
- $\rho_l$ : Density of liquid droplet
- v: Specific volume

In order to carry out simulations to optimise dropwise condensation behaviour as part of WP6, correlations between parameters need to be identified on which to base models, subject to agreement from the advisory board.

The heat transfer will be limited by the total thermal resistance at the surface, which can be expressed by the difference between the vapour saturation temperature ( $T_{sat}$ ) and the wall temperature ( $T_w$ ). The thermal resistance can be broken into constituent parts, based on the heat transfer through an isolated drop, as expressed by Sikarwar et al (2013):

Date: 28 February 2020

- Conduction resistance: Temperature difference as a result of conduction heat transfer through the drop ( $k_l$  is the thermal conductivity of the liquid droplet):

$$\Delta T_{cond} = \frac{q_d r (1 - \cos \theta_{avg})}{4\pi r^2 k_l} \quad [23]$$

- Film resistance: Temperature difference as a result of the vapour-liquid interface:

$$\Delta T_{int} = \frac{q_d}{2\pi r^2 h_{int} (1 - \cos \theta_{avg})} \quad [24]$$

- Curvature resistance: Temperature difference arising from the curvature of the drop free surface (Carey, 1992):

$$\Delta T_{curv} = \left(\frac{2\sigma}{r}\right) \left(\frac{v_l T_w}{h_{lv}}\right) = \frac{(T_{sat} - T_w) r_{min}}{r} \quad [25]$$

- Coating resistance: Temperature difference arising from the coating material applied on the substrate ( $\delta$  is the thickness of the coating):

$$\Delta T_{coat} = \frac{q_d \delta}{k_{coat} \pi r^2 (1 - \cos^2 \theta_{avg})} \quad [26]$$

- Constriction resistance: This parameter measures the effect of surface thermal resistance on DWC. Although contested in literature, the effect arises as a result of non-uniform heat flux distribution over the condensing surface, as described by Mikic (1969):

$$R_{const} = \frac{8}{3\pi k_w} \sum_{r_{min}}^{r_{max}} \frac{n_r r^3}{[1-f(r)]} \quad [27]$$

where

$$\Delta T_{curv} = \frac{q_d}{R_{const}} \quad [28]$$

These equations can be combined to give the heat transfer as dependent on the droplet radius ( $r$ ), the heat transfer at the liquid-vapour interface ( $h_{lv}$ ) and the droplet contact angle ( $\theta$ ):

$$q_d = (\pi r^2 \rho_l h_{lv}) \cdot (2 - 3 \cos \theta + \cos^3 \theta) \cdot \left(\frac{dr}{dt}\right) \quad [29]$$

These equations can be manipulated to obtain the drop growth rate,  $\frac{dr}{dt}$ .

Sikarwar et al (2013) also developed a model of droplet coalescence based on studying this phenomenon using high speed cameras. A critical droplet radius has to be achieved in order for coalescence to occur. This radius is that which would exist for a droplet which encompassed the total volume of the two droplets coalescing i.e. the radius of the droplet after coalescence has occurred. This is dependent on the average contact angles of the two droplets:

$$r_c = \left[ \frac{3(V_i + V_j)}{\pi(2 - 3 \cos \theta_{avg} + \cos^3 \theta_{avg})} \right]^{\frac{1}{3}} \quad [30]$$

## **7 SCIENTIFIC LITERATURE ON SUPERHYGROPHOBIC COATINGS**

### **7.1 Overview**

There are many scientific papers investigating various surface structures and the role they play in the development of superhydrophobicity (McHale et al 2004; Parkin and Palgrave, 2005; Perro et al, 2005; Roach et al, 2008; Latthe et al, 2012). Such behaviour is expected to lead to products which do not suffer from ice-formation (Wang et al, 2007), and have significantly reduced levels of fouling during operation (Marmur, 2006). It is also expected to improve fluid flow over surfaces and have applicability in textiles. The majority of the approaches attempted recognise the need for dual scale roughness for the development of superhydrophobicity (Shirtcliffe et al, 2004; Tawfick et al, 2012 ). Tuteja et al (2008) have published widely on the topic of surface roughness, their key findings being that both micro and nano-scale features are necessary for high static contact angles and low contact angle hysteresis to be achieved.

The key aspects of the work reported in the scientific literature are:

- Methodologies to introduce roughness into surfaces.
- Development of an understanding of the key design rules determining repellent behaviour.
- Identification of materials/roughness combinations which give the highest contact angle (most often with water as the liquid) and the lowest contact angle hysteresis/roll-off angle.
- Consensus that current approaches to generating roughness lead to mechanically fragile surfaces which lack durability and can readily be damaged.

### **7.2 Roughness generation: top-down/bottom up approaches**

There are two generic approaches to the creation of roughness in surfaces to enable superhydrophobic behaviour: top-down engineering based methods and bottom-up synthesis. The top-down approaches are based on breaking down larger materials to give the desired structures; bottom-up approaches are based on self-assembly methods or chemical synthesis approaches. Both these approaches are widely used in the field of nanotechnology for the fabrication of nanomaterials and nanostructures, Figure 9.

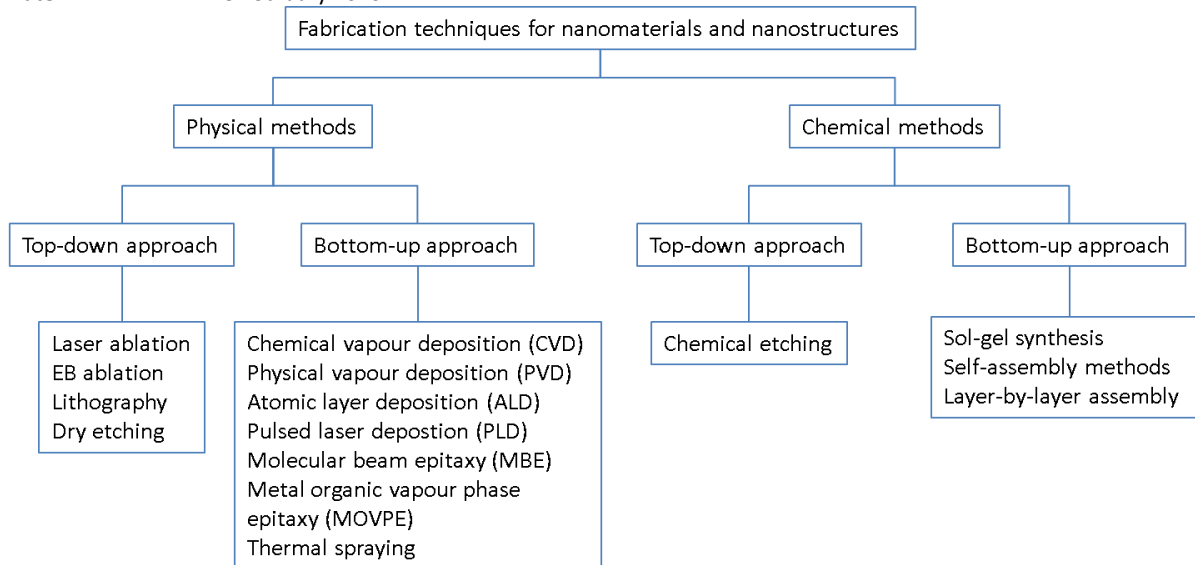


**Figure 9** Techniques used to prepare manufactured nanomaterials and nanostructures.

For the preparation of a superhydrophobic surface, the generic approaches are to either introduce the requisite structure into a material with inherent water repellent characteristics or to apply a low energy ( $\gamma_s < 22 \text{mN/m}$ ) treatment to a textured surface. In the second case it is essential that this treatment does not planarise the surface and so negate the texture.

Within the scientific literature the various descriptors for highly repellent surfaces yield a very large number of hits (>50,000). Refinement to more manageable numbers can be achieved via the selection of key terms, but it should be recognised that the underpinning principles behind functional efficacy must be considered when reviewing many of the reported approaches with a view to adopting methods to address a specific application and performance specification.

Within the GeoHex project the substrates of interest are steel, aluminium and copper. Below is a brief review of a selection of relevant papers that may provide guidance towards to the preparation of materials and surfaces for this project.

### 7.3 Steel substrates

With regards to steel substrates many of the papers in the literature are about the impact of superhydrophobic behaviour on the corrosion characteristics of steel. Notable among these papers are Ejenstam et al (2013), Qing et al (2015), Latthe et al (2015), Guo et al (2012), Weisensee et al (2014) and Zhang et al (2016).

These papers have a common characteristic in the sense that they identify that superhydrophobic behaviour appears to retard the rate or degree of corrosion. They appear to indicate that the reduction in the diffusion of ions to the surface of the metal due to the presence of entrapped air is an important consideration in the corrosion behaviour.

- Latthe et al (2015) is a useful review of superhydrophobicity and describes a simple methodology for producing a superhydrophobic surface by creating a rough finish with a low energy coating:
  - They etched stainless steel to provide the requisite roughness and then immersed the material in a methylchlorosilane/hexane solution.

- They note that very high static water contact angles are achieved and remain even after bending of the stainless steel substrates. However, the contact angle hysteresis increases with increasing damage to the surface leading to reduced self-cleaning behaviour.
  - They concluded that the superhydrophobic surface acts as a physical barrier between the metal and the environment, offering improved corrosion resistance.
  - The central conclusion to this review is that while achieving superhydrophobicity by mimicking biological structures can be readily achieved, retention of the full set of required behaviours has proved elusive, even under relatively benign conditions. Specifically, they show that while superhydrophobic behaviour can be demonstrated even after bending, relatively large cracks (~1µm) appear in the coating providing opportunity for the creation of corrosion pathways.
  - They also indicate that challenges to industrialisation include large-scale application and supply/supply chain considerations.
- Qing et al (2015) reviewed the drivers for the development of superhydrophobic coatings for steel and identified a number of recent approaches. They highlighted the challenging and potentially time consuming and expensive approaches to achieving such behaviour:
    - Their favoured approach was to modify ZnO nanoparticles with stearic acid and to incorporate them into a fluorinated siloxane as a binder.
    - They commented that the hydrophobic properties were improved by the roughness created by the ZnO particles.
    - One of the attempted formulations was easily removed under light finger pressure. Their best mixture coating was described as durable, but no details supporting this were provided.
- Ejenstam et al (2013) reviewed the impact of surface morphology on behaviour and concluded that a stable Cassie-Baxter state is the most promising.
    - The fabrication approach adopted in this case was an abrasive surface roughening followed by deposition of a wax coating.
    - The authors noted that the durability of the coating needed improving to enable application in an aggressive wear environment.
- Guo et al (2012) present a method for growing a superhydrophobic layer on a carbon steel substrate. They based their approach on the combination of physical and chemical treatment of the surface and emphasised the ease of application of their process.
    - They used an electroless galvanic deposition process to grow a three-level hierarchical multi-scale structure (present as micro- and nano-flower and particle structures).
    - They then use a fluorinated silane to chemically treat the surface of the textured copper layer.
    - The obtained layer shows water contact angles of up to 166° with a roll-off angle of less than 2°
- Weisensee et al (2014) investigated the hydrophobic and oleophobic behaviour of steel substrates with metallic micro-mushroom re-entrant structures in various sizes and distributions.
    - The re-entrant structures were created using micro electrical discharge machining.
    - The influence of the different dimensions of the micro-mushrooms on the resulting contact angle (with water, oil and isopropyl alcohol) was investigated.
    - None of the studied geometries showed superhydrophobic behaviour coupled to superoleophobic behaviour.
- The use of superhydrophobic behaviour to enable the separation of oil and water is described by Lu et al (2014).

## 7.4 Copper substrates

- Liu et al (2014) cover the surface modification of a copper substrate by electrodeposition of cerium salts and subsequent chemical treatment with myristic acid. The formed cerium myristates provide the surface with superhydrophobic properties.
- Mohamed et al (2015) provide a useful review of corrosion behaviour of superhydrophobic surfaces. They describe the basic concept as the provision of features that entrap air preventing the migration of ions to the copper substrate, Figure 10.

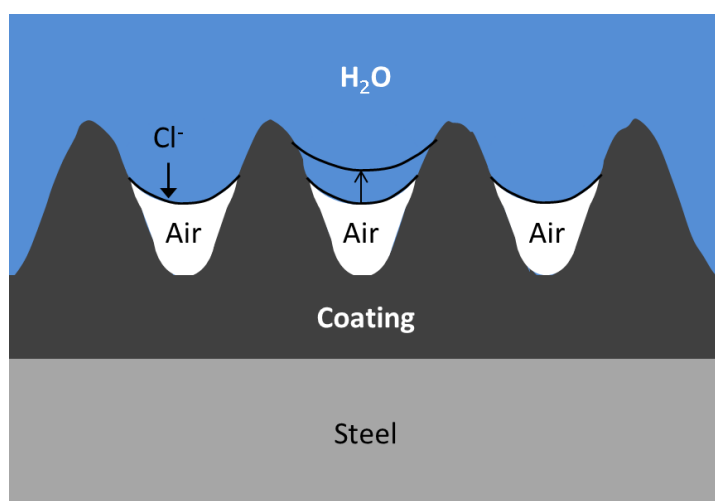


**Figure 10** Model of the interface between superhydrophobic surface and corrosive seawater. The Cl<sup>-</sup> ions can barely reach the bare surface because of the entrapped air (after Mohamed et al, 2015).

- The use of nanostructured superhydrophobic copper surfaces to promote dropwise condensation of steam and high droplet mobility is discussed in detail by Torresin et al (2013). They also specifically highlight the Cassie-Baxter to Wenzel transition indicating penetration of the topographic features leading to lower drop mobility. They emphasise the need for testing under stringent conditions representative of the operational environment.
- Electric brush plating methods and a subsequent stearic acid treatment has recently been described as providing superhydrophobic behaviour to copper films (Meng, et al., 2019).

## 7.5 Aluminium substrates

- A useful review of chemical etching processes for aluminium substrates is provided by Peng and Bhushan (2016). They also describe subsequent silane treatments to generate superoleophobic surfaces, which demonstrate superhydrophobic static contact angles when the liquid is hexadecane. Contact angle hysteresis and roll-off angles are also low and indicate a very high level of repulsion to this liquid.

## **8 ENHANCEMENT METHODS SPECIFIC TO GEOHEX**

### **8.1 Superhydrophobic and superoleophobic surfaces with CuO nanostructures**

Ujjain et al (2016) used a chemical bath deposition (CBD) technique to synthesize a range of different CuO morphologies on a steel substrate, including spherical, needle and hierarchical cauliflower morphologies. The differences in morphology of nanostructures was as a result of varying the concentration of sodium dodecyl sulfate solutions (containing cupric sulphate). Poly(dimethylsiloxane) (PDMS) was used as a low surface energy material to transform hydrophilic CuO nanostructures to become hydrophobic. Each of the nano-textured morphologies reported had a very high water contact angle after coating in PDMS, up to  $163^\circ$  and very low contact angle hysteresis ( $\Delta\theta \approx 2^\circ$ ). They also showed superoleophobic behaviour, with the hierarchical cauliflower exhibiting the highest contact angles in glycerol ( $160^\circ$ ).

### **8.2 Superhydrophobic and superoleophobic surfaces with TiO<sub>2</sub>/ZnO nanoparticles for condensation**

Metallic oxides have been found to be promising materials to use as part of hierarchical structures to give good hydrophobic and oleophobic properties. Tu et al (2018) sprayed an emulsion of waterborne perfluoroalkyl methacrylic copolymer (PMC) mixed with TiO<sub>2</sub> onto a wood substrate coated with PDMS. This was found to be a relatively simple technique to give a durable coating with superhydrophobic and superoleophobic properties with a contact angle of around  $150^\circ$  in various liquids. Wang et al (2010) also reported high surface contact angles in oil based liquids (e.g.  $155^\circ$  in hexadecane) using hierarchical surface textures containing titanium dioxide nanostructures. Aligned TiO<sub>2</sub> nanotubes were formed on laser micromachined micropillars of titanium. Macias-Montero et al (2019) reported similar findings from titanium dioxide nanotubes which promoted DWC.

Zinc oxide has also been reported to have similar effects. In a similar study to Tu et al (2018), Steele et al (2009) used a composite containing ZnO and PMC on a glass slide, which led to hierarchically structured surfaces with a contact angle of  $154^\circ$  and  $\Delta\theta \approx 6^\circ$ . Brockway and Taylor (2017) synthesised zinc-oxide based films onto aluminium substrates with a tuneable level of nanoporosity through varying the temperature and concentration of the immersion bath containing zinc nitrate and hexamine. After silanization of the surface to give a hydrophobic surface, they achieved contact angles of up to  $178^\circ$  in water, whilst also exhibiting superoleophobic properties (contact angle of  $124^\circ$  in dipropylene glycol). They also performed condensation studies, showing that the surface with the highest contact angle did not lead to the best condensation performance, with large droplets forming which became pinned to the surface. Instead, a surface with a slightly finer pore size and varied morphology gave sustained droplet-shedding, with a droplet diameter reported to be less than 1mm. Further work could be undertaken to study the relationship between pore morphology and condensation behaviour.

### **8.3 Functional hierarchical mesh-covered surfaces**

Recent surfacing techniques employed to increase the condensation heat transfer properties include the use of meshes. Surface conditioned interweaving micro-networks, for example nanostructured copper micro-meshes, have previously been used in several applications, for example separating oil and water mixes (Gao et al, 2016) and have been used to improve boiling heat transfer properties (Cho et al, 2016). In terms of hydrophobic properties, a teflon-coated copper mesh was found to have an advancing contact angle and contact angle

hysteresis of water comparable to that of similar Teflon-coated nanostructures (Weisensee et al, 2015). Similarly TiO<sub>2</sub> nanoparticles sprayed onto silicon or stainless steel mesh substrates were found to have superoleophobic properties. The major benefit of hierarchical mesh-covered surfaces, however, is their ability to sustain very efficient drop-wise condensation to a large degree of supercooling (Wen et al, 2018).

One of the common problems in drop-wise condensation applications is that the droplet surface coverage in the steady state condition is quite high, limiting the amount of new droplets that can condense and ensure a high heat transfer. On a vertical surface, gravity has to be relied upon to remove droplets. However, some superhydrophobic nanostructured surfaces have been reported as showing an improved heat transfer through a droplet ‘jumping’ mechanism. Adjacent droplets can coalesce; the energy obtained from the reduction in surface energy can be used as kinetic energy to remove the droplet from the surface, freeing up space for new droplets to form on the surface (Boreyko and Chen, 2009). This mechanism is dependent on surface roughness; the mobile Cassie state is required, as opposed to the Wenzel state (Wen et al, 2017). (i.e. droplet sitting on top of rough surface, as opposed to flowing into the roughness of the surface). A schematic of this mechanism is shown in Figure 11.

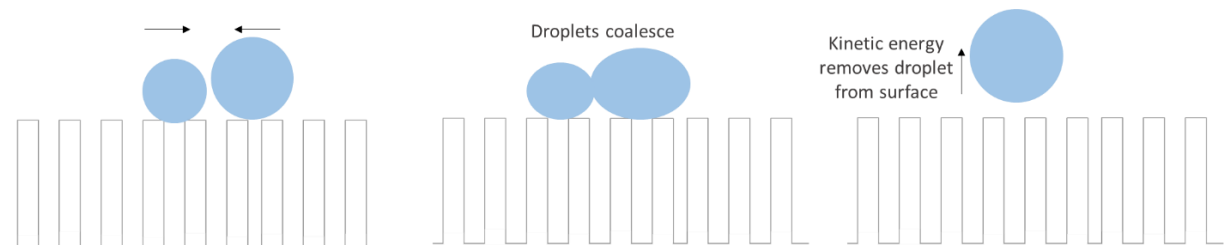


**Figure 11** Schematic illustrating the droplet jumping mechanism of removal of droplets from a hydrophobic surface

However, at high supercooling, this mechanism breaks down. Droplets are able to condense within the nanostructures, leading to subsequent flooding, greatly reducing the heat transfer properties.

An alternative mechanism enables long-range coalescence of droplet condensates, as first reported on gold nanowire arrays (Anderson et al, 2012). Droplets which condense on the surface can be drawn through the micropores within the surface into a liquid film layer running through interconnected pores within the mesh structure. This could then flow away, for example channelled into one larger droplet some distance from the original droplet. This leads to a smaller number of large droplets, with the remaining surface free for subsequent droplets to condense. A schematic illustrating the mechanism is shown in Figure 12. Recent work has demonstrated that very finely spaced hierarchical nanostructures can improve droplet jumping (Wang et al, 2017; He et al, 2016) leading to enhanced condensation heat transfer.

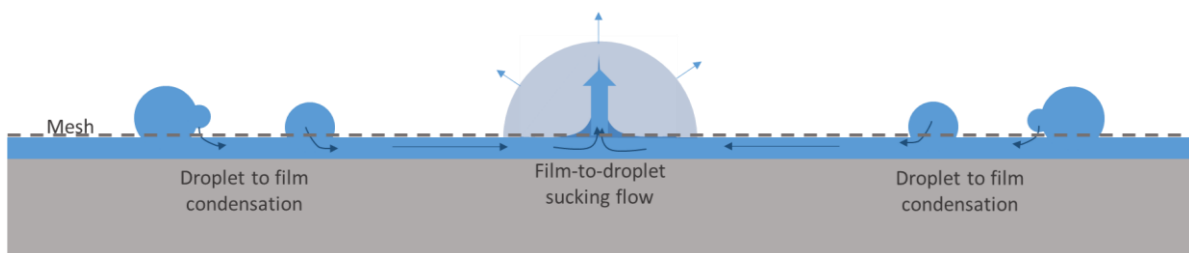


**Figure 12** Schematic illustrating the sucking flow mechanism of removal of droplets from a hierarchical hydrophobic surface

Wen et al (2018) used commercially available copper mesh (65 $\mu$ m thick wire (d), 65-195 $\mu$ m spacing (w)) bonded onto a plain copper substrate, with CuO nano-structures applied onto the substrate and mesh surface using self-limiting chemical oxidation. This was compared to a plain hydrophobic surface and a nanostructured superhydrophobic surface. They found this surface promoted a 'sucking flow' mechanism as described above. This allowed a rapid removal of droplets through the high volume of micropores in the meshed surface and channelled into one large droplet. However, this led to an overall lower average droplet size and decreased amount of time that droplets remained on the surface, leading to a low overall percentage surface coverage, allowing a fresh surface for condensation to occur again. The average droplet departure radius was approximately 1mm. In terms of the droplet dynamic behaviour, mesh with w/d=3 was found to perform better than mesh with w/d=1 or w/d=2.

These findings were backed up in that the meshed surfaces showed a comparable or higher heat flux than the plain hydrophobic or nanostructured superhydrophobic surfaces. At low surface supercooling, the nanostructured hydrophobic surface performed equally well, but at higher supercooling, this dropped off dramatically compared to the meshed surface due to flooding events. The good performance of the mesh layer was consistent even up to a supercooling of 30K. Mesh with w/d=1 performed best at low supercoolings (where a jumping mechanism was favoured as smaller and deeper micropores are provided) whereas w/d=3 performed best at high supercoolings (above 4.5K) where a sucking flow mechanism performed better as larger channels allow high flow rates. At a supercooling of 0.7K, there was a 254% increase in the heat transfer coefficient compared to the plain hydrophobic surface and a 53% increase at a 28.1K supercooling.

Further progress is possible, however, through careful control of the channels within the surfacing layer to maximise the sucking flow behaviour and a reduction of the droplet departure diameter (Chen and Wang, 2018).

#### **8.4 Robust hydrophobic/oleophobic amorphous metal coatings**

In order to produce a surface or coating on a substrate that has a higher mechanical strength and durability, there is an incentive to use metallic materials. However, these have an inherently high surface energy, leading to low contact angles which do not act to promote drop wise condensation. Metallic glasses have attracted attention more recently. Although they do not exhibit a low surface energy naturally, there is potential to form hierarchical structures which can reduce the surface contact angle considerably. They also show a high hardness, strength and corrosion resistance which give the potential to form a durable, stable hydrophobicity. These properties are of particular interest in heat exchanger applications, where physical and chemical durability are very significant.

For example, the wetting behaviour of Ce- and CaLi-based bulk metallic glasses showed that hydrophobicity was obtained after low surface energy modification of a hierarchical surface structure (Wang, 2009, Liu et al, 2011). Similarly, palladium-based metallic glasses have shown similar results. For example, Xia et al (2012) formed a Pd<sub>40</sub>Cu<sub>30</sub>Ni<sub>10</sub>P<sub>20</sub> bulk metallic glass through vacuum induction melting and copper mould casting. Deep reactive ion (DRI) etching and hot embossing were used to produce a 100 $\mu$ m deep honeycomb surface texture using a silicon mould. A high surface contact angle was found, with a maximum with an increasing honeycomb pitch. For example, a contact angle of around 152° was reported with a honeycomb pitch of 600 $\mu$ m compared to 98° for a smooth metallic glass surface and 131° for a honeycomb pitch of 100 $\mu$ m. It was theorised that the trapped air within the honeycomb structure gave the superhydrophobic effect a good stability.

A similar metallic glass (Pd<sub>43</sub>Ni<sub>10</sub>Cu<sub>27</sub>P<sub>20</sub>) was formed by Arora et al (2013) with a nanorod structure using thermoplastic processing with an alumina mould in the supercooled liquid region above the glass transition temperature. This was compared to a nanostructured nickel-based metallic glass (Ni<sub>60</sub>Pd<sub>20</sub>P<sub>17</sub>B<sub>3</sub>) formed

through an electrochemical process (three electrode set-up with an acidic medium). The surface texturing increased the contact angle from 70° to 110° and from 84° to 112° for the nanorod and nanostructured surfaces, respectively.

Cheng et al (2010) illustrated a similar effect in amorphous NiP coatings and applied this to heat transfer. These coatings are known to have good corrosion and wear properties (Ashassi-Sorkhabi and Rafizadeh, 2004; Narayanan et al, 2006). Various composition coatings with a spherical nodular surface texture (around 10µm diameter nodules) were deposited using electroless plating. Drop-wise condensation was observed; the sample with the least amount of nanocrystalline phase showed the highest heat transfer coefficient, which was over double that from the uncoated substrate. Moreover, this same had the smallest droplet size and the highest shedding frequency. Further work should be undertaken to optimise the electroless plating process and study the effect of amorphous metallic coatings for heat transfer over a range of conditions and undercoolings.

## 9 SUMMARY

This review discussed the characteristics of ideal surfaces for condensation heat transfer, with water as well as low surface energy fluids, e.g. ORC working fluids, with a specific focus on enhancement of DWC. The effects of surface energy and texture, in relation to DWC, have also been reviewed, along with correlations between condensation heat transfer and physical parameters, e.g. droplet radius. The main findings from the review were:

- The ideal characteristic for condensation heat transfer enhancement will be that heat transfer surfaces have a high degree of hydrophobicity. The underpinning principles behind the formation of superhydrophobic surfaces is relatively well understood, from the perspective of having a surface that is a composite of the solid and entrapped air. However, the design rules to achieve such conditions is not well understood, particularly in relation to fluids other than water.  
Ideal surfaces will have surface chemistries that minimise electrostatic interactions and formal reactions between the solid and the liquid. Ideal surfaces will also have topographic features that enable entrapped air to act as a structural part of the composite surface.
- Correlations for condensation heat transfer have been reviewed and the validity of these correlations will be tested against the data generated in the GeoHex project.

Most of the literature is focussed on the repulsion of water and the discussion centres around superhydrophobicity. Other liquids of interest tend to be hydrocarbon oils and so there is a smaller, but significant corpus of work on oleophobicity. The typical surface tension of liquid hydrocarbons is <20mN/m. Very high levels of repellency to liquids with surface tension values of <10mN/m are rarely reported. The potential of these liquids to fill textured surfaces is very high and so most of the textures that adopt Cassie-Baxter behaviour for higher surface tension liquids will transition to Wenzel with such low surface tension liquids. There are some emerging reports however, such as the article by Pan et al (2018).

The key challenges facing the GeoHex project are the design and development of surface topographies on the target substrates and the modification of the surface chemistry to provide the necessary surface energy for the solid. This will lead to promotion of dropwise condensation, leading to a high heat transfer. The retention of this behaviour for the lifetime of the heat exchanger for condensing water is central to success for the steam condenser. The challenge for the dropwise condensation of R134a, which has a surface tension of 8.37mN/m, is more fundamental. Achieving super-repulsion to this chemical will require far higher performance than has

been reported in the literature. However, the indications from the literature are clear, managing the structural aspects of the surface will be key to achieving this goal.

## 10 REFERENCES

Abu-Orabi, 1998: 'Modeling of heat transfer in dropwise condensation'. *International Journal of Heat and Mass Transfer*, Vol. 41, Issue 1, pp81-87.

Anderson D, Gupta M, Voevodin A, Hunter C, Putnam S, Tsukruk V and Fedorov A, 2012: 'Using amphiphilic nanostructures to enable long-range ensemble coalescence and surface rejuvenation in dropwise condensation'. *ACS Nano*, Vol 6, Issue 4, pp3263-3268.

Arkles B, 2006: 'Hydrophobicity, Hydrophilicity and Silanes'. *Paint & Coatings Industry*, Issue 114-124.

Arora H, Xu Q, Xia Z, Ho Y, Dahotre N, Schroers J and Mukherjee S: 'Wettability of nanotextured metallic glass surfaces'. *Scripta Materialia* vol. 69, pp732-735.

Ashassi-Sorkhabi H and Rafizadeh S, 2004: 'Effect of coating time and heat treatment on structures and corrosion characteristics of electroless Ni-P alloy deposits.' *Surface and Coatings Technology*, Vol. 176, Issue 3, pp318-326.

Bisetto A, Torresin D, Tiwari M, Del Col D and Poulikakos D, 2014: 'Dropwise condensation on superhydrophobic nanostructured surfaces: literature review and experimental analysis'. *Journal of Physics: Conference Series* 501 (2014).

Boreyko J and Chen C, 2009: 'Self-propelled dropwise condensate on superhydrophobic surfaces'. *Physical Review Letters*, Vol. 103, Issue 18-30, October 2009.

Brockway L and Taylor H, 2017: 'A nanoporous, ultrahydrophobic aluminum-coating process with exceptional dropwise condensation and shedding properties'. *Materials Research Express*, 4, 4.

Carey V, 2007: 'Liquid Vapor Phase Change Phenomena: An Introduction to the Thermophysics of Vaporization and Condensation Processes in Heat Transfer Equipment, Second Edition'. CRC Press, Florida, US. ISBN 9781591690351

Cassie, B and Baxter S, 1944: 'Wettability of porous surfaces.' *Trans. Faraday. Soc.*, 40(5), pp. 546-551.

Chen Y and Wang Z, 2018: 'New approach for efficient condensation heat transfer'. *National Science Review*, Vol. 6, Issue 2, pp185-186.

Cheng L, Cheng Y, Xin G and Zou Y, 2010: 'Influence of Ni-P coating microstructure of condensation heat transfer.' *Proceedings of the 14<sup>th</sup> International Heat Transfer Conference, IHTC14*, August 2010.

Cho J, Preston D, Zhu Q and Wang E, 2016: 'Nanoengineered materials for liquid-vapour phase-change heat transfer.' *Nature Reviews: Materials*, Vol. 2, 16092.

Ejenslam L, Ovaskainen L, Rodriguez-Meizoso I, Wagberg L, Pan J, Swerin A and Claesson P, 2013: 'The effect of superhydrophobic wetting state on corrosion protection—The AKD example'. *Journal of Colloid and Interface Science*, Vol. 412, pp56-64.

**Document:** D1.3 Ideal flow boiling surface for ORC

**Version:** 1.0

**Date:** 28 February 2020

ElSherbini, A and Jacobi A, 2006: 'Retention forces and contact angles for critical liquid drops on non-horizontal surfaces.' *Journal of Colloid and Interface Science*, Volume 299, pp. 841-849.

Extrand W and Gent N, 1990: 'Retention of liquid drops by solid surfaces.' *Journal of Colloid And Interface Science*, 138(2), pp. 431-442.

Extrand W and Kumagai Y, 1995: 'Liquid drops on an inclined plane: The relation between contact angles, drop shape, and retentive force'. *Journal of Colloid and Interface Science*, 170(2), pp. 515-521.

Fowkes F, 1964: 'Attractive forces at interface.' *Ind. Eng. Chem*, Issue 40-52.

Gao C, Zhou J and Du R, 2016: 'Robust superhydrophobic foam: a graphdiyne-based hierarchical architecture for oil/water separation.' *Advance Materials* 2016, Vol. 28, pp 168-173.

Guo F, Su X, Hou G, Li, 2012: 'Bioinspired fabrication of stable and robust superhydrophobic steel surface with hierarchical flowerlike structure'. *Colloids and Surfaces A: Physicochemical and Engineering Aspects* 401, 61-67.

He M, Ding Y, Chen J and Song Y, 2016: 'Spontaneous uphill movement and self-removal of condensates on hierarchical tower-like arrays'. *ACS Nano*, 2016, Vol. 10.

Johnson R and Dettre R, 1964: 'Contact angle hysteresis: I. Study of an idealized rough surface'. *Advances in Chemistry*, Vol. 43, pp112-135

Khan S, Tahir F, Baloch A and Koc M, 2019: 'Review of micro-nanoscale surface coating application for sustaining dropwise condensation'. *Coatings* 2019, Vol. 9, 117.

Koch K and Barthlott W, 2009; 'Superhydrophobic and superhydrophilic plant surfaces: an inspiration for biomimetic materials'. *Phil. Trans. R. Soc. A* Vol 367, 1487–1509

Krasovitski B and Marmur A, 2005: 'Drops down the hill: theoretical study of limiting contact angles and the hysteresis range on a tilted plate'. *Langmuir*, 21, 9 pp3881-3885.

Latthe S S, Gurav A B, Maruti C S and Vhatkar R S, 2012: 'Recent Progress in Preparation of Superhydrophobic Surfaces: A Review'. *Journal of Surface Engineered Materials and Advanced Technology*, 2012, 2, 76-94.

Latthe S S, Sudhagar P, Devadoss A, Kumar A, Liu S, Terashima C, Nakata K, Fujishima A, 2015: 'A mechanically bendable superhydrophobic steel surface with self-cleaning and corrosion-resistant properties'. *Journal of materials chemistry. A, Materials for energy and sustainability* 3.27 14263-14271.

Lautrup B, 2010: 'Surface tension' in 'Physics of Continuous Matter: Exotic and Everyday Phenomena in the macroscopic world.' CRC Press.

Lee S, Park J and Lee R, 2008: 'The wettability of fluoropolymer surfaces: Influence of surface dipole.' *Langmuir*, Volume 24, pp. 4817-4826.

Li Y, Men X, Zhu X, Ge B, Chu F, Zhang Z, 2016: 'One-step spraying to fabricate nonfluorinated superhydrophobic coatings with high transparency'. *Journal of Materials Science*, 51, pp2411-2419.

Liu K, Li Z, Wang W and Jiang L, 2011: 'Facile creation of bio-inspired superhydrophobic Ce-based metallic glass surfaces'. *Applied Physics Letters*, vol. 99, 261905.

Liu Y, Li S, Zhang J, Wang Y, Han Z and Ren L, 2014: 'Fabrication of biomimetic superhydrophobic surface with controlled adhesion by electrodeposition'. *Chemical Engineering Journal*, Vol. 248, pp440-447.

Lu Y, Sathasivam S, Song J, Chen F, Xu W, Carmalt C and Parkin I, 2014: 'Creating superhydrophobic mild steel surfaces for water proofing and oil-water separation.' *Journal of Materials Chemistry A*, Volume 2, p. 1162811634.

Ma M and Hill R, 2006: 'Superhydrophobic surfaces. *Current Opinion in Colloid & Interface Science*', Volume 11, p. 193–202.

Macias-Montero M, Lopez-Santos C, Filippin A, Roco V, Espinos J, Fraxedas J, Perez-Dieste V, Escudero C, Gonzalez-Elipe A and Borrás R, 2017: 'In situ determination of the water condensation mechanisms on superhydrophobic and superhydrophilic titanium dioxide nanotubes.' *Langmuir* 2017, Vol. 33, 26, pp6449-6456.

Makkonen L, 2016: 'Young's equation revisited.' *Journal of Physics: Condensed Matter*, 28(13), p.135001.

Makkonen L, 2017: 'A thermodynamic model of contact angle hysteresis.' *The Journal of Chemical Physics*, 147(6), p.064703

Marmur A, 2006: 'Underwater superhydrophobicity; theoretical feasibility. *Biofouling* 22(2) 107-115.

Marmur A, 2012: 'Hydro- hygro- oleo- omni-phobic? Terminology of wettability classification. *Soft Matter*, 2012, 8, 6867

McHale G, Shirtcliffe N J, Aqil S, Perry C C, Newton M. I, 2004: 'Topography driven spreading'. *Phys. Rev. Lett.* 93, 2004, Art. No. 036102.

Meng K, Tan X, Shang F and Jiang Z, 2019: 'A universal method to fabricate copper films with superhydrophobic and anti-corrosion properties.' *Materials Science and Technology*, 35(6), pp. 695-701.

Mikic B, 1969: 'On mechanism of dropwise condensation'. *International Journal of Heat and Mass Transfer*, Vol. 12, Issue 10, pp1311-1323.

Miljkovic N and Wang E, 2017: 'Condensation heat transfer on superhydrophobic surfaces'. *MRS Bulletin* 38, no. 05, pp397-406.

Mohamed A, Abdullah A, Younan N, 2015: 'Corrosion behavior of superhydrophobic surfaces: A review'. *Arabian Journal of Chemistry*, Vol. 8, Issue 6, pp749-765.

Narayanan S, Baskaran I, Krishnaveni K and Shanmugam P, 2006: 'Deposition of electroless Ni–P graded coatings and evaluation of their corrosion resistance' *Surface and Coatings Technology*, 200(11), pp3438-3445.

Owens D and Wendt R, 1969: 'Estimation of the surface free energy of polymers.' *J. Appl. Polym. Sci*, Issue 1741-1747.

Pan S, Guo R, Bjornmalm M, Richardson J, Li L, Peng C, Bertleff-Zieschang N, Xu W, Jiang J and Caruso F, 2018: 'Coatings super-repellent to ultralow surface tension liquids'. *Nature Materials*, Volume 17, pp. 1040-1047.

Parkin I P and Palgrave R G, 2005: 'Self-cleaning coatings'. *J. Mater. Chem.*, 15, 1689–1695.

Peng S and Bushan B, 2016: 'Mechanically durable superoleophobic aluminium surfaces with microstep and nanoreticula hierarchical structure for self cleaning and antismudge properties.' *Journal of Colloid and Interface Science*, Volume 461, pp. 276-284.

**Document:** D1.3 Ideal flow boiling surface for ORC

**Version:** 1.0

**Date:** 28 February 2020

Perro, A, Reculosa, S, Ravaine, S, Bourgeat-Lami, E Duguet, E, 2005: 'Design and synthesis of Janus micro- and nanoparticles'. *J. Mater. Chem.*(2005) 15, 3745–3760.

Qing Y, Yang C, Hu C, Zheng Y and Liu C, 2015: 'A facile method to prepare superhydrophobic fluorinated polysiloxane/ZnO nanocomposite coatings with corrosion resistance'. *Applied Surface Science*, Vol. 326, pp48-54.

Quére D and Reyssat M, 2008: 'Non-adhesive lotus and other hydrophobic materials.' *Phil. Trans. R. Soc. A*, Volume 366, p. 1539–1556.

Ranieri S, Bozzoli F and Pagliarni G, 2009: 'Effect of a Hydrophobic Coating on the Local Heat Transfer Coefficient in Forced Convection under Wet Conditions'. *Experimental Heat Transfer*, Vol. 22, Issue 3, pp163-177.

Roach P, Shirtcliffe N J, Newton M I, 2008: 'Progress in Superhydrophobic Surface Development'. *Soft Matter*, 2008, 4 (2), 224-240.

Schmidt E, Schurig W and Sellschopp W, 1930: 'Versuche über Kondensation von Wasserdampf in Film- und Tropfenform'. *Technische Mechanik und Thermodynamik*, Vol. 1, Issue 2, pp 53-63.

Shirtcliffe N, McHale G, Newton M, Chabrol G, Perry C, 2004: 'Dual scale roughness produces unusually water repellent surfaces.' *Advanced Materials*, Issue 1929-1932.

Sikarwar B, Khandekar S and Muralidhar K, 2013: 'Mathematical modelling of dropwise condensation on textured surfaces'. *Sadhana*, Vol. 38, Part 6, pp 1135-1171.

Steele A, Bayer I and Loth E, 2009: 'Inherently superoleophobic nanocomposite coatings by spray atomisation'. *Nano Letters*, Vol. 9, pp501-505.

Tawfik S, De Volder M, Copic D, Park S J, Oliver C R, Polsen E S, Roberts M J, Hart AJ; 2012: 'Engineering of micro and nanostructured surfaces with anisotropic geometries and properties.' *Adv. Mater.*, 24 (2012), pp.

Torresin D, Tiwari M, Del Col D and Poulikakos D, 2013: 'Flow condensation on copper-based nanotextured surfaces.' *Langmuir*, Volume 29, pp. 840-848.

Tu K, Kong L, Wang X and Guan H, 2018: 'Facile preparation of mechanically durable, self-healing and multifunctional superhydrophobic surfaces on solid wood. *Materials and Design*, 140, pp30-36.

Tuteja A, Choi W, Ma M, Mabry J M, Mazzella S A, Rutledge G C, McKinley G H and Cohen R E, 2008: 'Designing Superoleophobic Surfaces'. *Science* 318, 1618-1622.

Ujjain S, Roy P, Kumar S, Singha S and Khare K, 2016: 'Uniting Superhydrophobic, Superoleophobic and Lubricant Infused Slippery Behavior on Copper Oxide Nano-structured Substrates'. *Scientific Reports*, 6, 35524, October 2016.

Wang D, Wand X, Liu X and Zhou F, 2010: 'Engineering a titanium surface with controllable oleophobicity and switchable oil adhesion'. *Journal of Physical Chemistry C*, vol. 114, pp9938-9944.

Wang H, Tang L, Wu X, Dai W, Qiu Y, 2007: 'Fabrication and anti-frosting performance of super hydrophobic coating based on modified nano-sized calcium carbonate and ordinary polyacrylate'. *Applied Surface Science*, Vol. 253, Issue 22, pp8818-8824.

- Wang K, Liang Q, Jiang R, Zheng Y, Lan Z and Xuehu M, 2017: 'Numerical Simulation of Coalescence-Induced Jumping of Multidroplets on Superhydrophobic Surfaces: Initial Droplet Arrangement Effect'. *Langmuir*, vol. 33, issue 25, pp6258-6268.
- Wang W, 2009: 'Bulk metallic glasses with functional physical properties'. *Advanced Materials*, Vol. 21, pp4524-4544.
- Weisensee P, Neelakantan N, Suslick K, Jacobi A and King W, 2015: 'Impact of air and water vapour environments on the hydrophobicity of surfaces'. *Journal of Colloid and Interface Science*, vol. 452, pp177-185.
- Weisensee P, Terrealba E, Raleigh M, Jacobi A and King W, 2014: 'Hydrophobic and oleophobic re-entrant steel microstructures fabricated using micro electrical discharge machining'. *Journal of Micromechanics and Microengineering*, Vol. 24, No. 9.
- Wen R, Xu S, Dongliang Z, Lee Y and Ma X, 2017: 'Hierarchical superhydrophobic surfaces with micropatterned nanowire arrays for high-efficiency jumping droplet condensation'. *Applied Materials and Interfaces*, Vol. 9, 51, pp44911-44921.
- Wen R, Xu S, Zhao D, Yang L, Ma X, Liu W, Lee Y and Yang R, 2018: 'Sustaining enhanced condensation on hierarchical mesh-covered surfaces'. *National Science Review*, Vol. 5, pp 878-887, 2018.
- Wenzel R, 1936: 'Resistance of solid surfaces to wetting by water.' *Ind. Eng. Chem*, Issue 988-994.
- Xia T, Li N, Wu Y and Liu L, 2012: 'Patterned superhydrophobic surface based on Pd-based metallic glass'. *Applied Physics Letters*, vol. 101, 081601.
- Young T, 1805: 'An essay on the cohesion of fluids.' *Phil. Trans. R. Soc.*, Issue 65-87.
- Zhang D, Wang L, Qian H, Li X, 2016: 'Superhydrophobic surfaces for corrosion protection: a review of recent progresses and future directions'. *J. Coat. Technol. Res.* (2016) 13 (1), 11-29.